Nuclear Engineering and Technology 55 (2023) 2572–2577

Contents lists available at ScienceDirect

Nuclear Engineering and Technology

journal homepage: www.elsevier.com/locate/net

Original Article

A field determination method of D-T neutron source yields based on oxygen prompt gamma rays

Xiongjie Zhang [a, **], Bin Tang [a, *], Geng Nian [b], Haitao Wang [a], Lijiao Zhang [a], Yan Zhang [a], Rui Chen [a], Zhifeng Liu [a], Jinhui Qu [a]

[a] Engineering Research Center of Nuclear Technology Application(East China University of Technology), Ministry of Education, Nanchang, 330013, China
[b] Chenghua Monitoring Station of Chengdu Pollution Source Monitoring Center, Chengdu, 610000, China

ARTICLE INFO

Article history:
Received 25 November 2022
Received in revised form
9 February 2023
Accepted 9 March 2023
Available online 2 June 2023

Keywords:
N-γtransport equation
Oxygen prompt gamma rays
D-T neutron source
Neutron yield

ABSTRACT

A field determination method for small D-T neutron source yield based on the oxygen prompt gamma rays was established. A neutron-gamma transport equation of the determination device was developed. Two yield field determination devices with a thickness of 20 mm and 50 mm were made. The count rates of the oxygen prompt gamma rays were calculated using three energy spectra processing approaches, which were the characteristic peak of 6.13 MeV, the overlapping peak of 6.92 MeV and 7.12 MeV, and the total energy area. The R-square of the calibration curve is better than 94% and the maximum error of the yield test is 5.21%, demonstrating that it is feasible to measure the yield of D-T neutron source by oxygen prompt gamma rays. Additionally , the results meet the requirements for field determination of the conventional D-T neutron source yield.

1. Introduction

The neutron source of the small D-T accelerator (D-T neutron source) is an important tool in performing application technology research on neutron physics and neutrons. It has the characteristics of high controllability and good monochromaticity, and has been widely appreciated by countries all over the world. Neutron logging technology using small D-T neutron sources has always been the representative of international advanced nuclear geophysical technology. In the field of petroleum exploration, neutron logging technology has become a high-level dynamic reservoir monitoring technology [1–6]. In the field of uranium exploration, neutron logging technology based on uranium fission, is a revolutionary nuclear logging technology for direct uranium determination that can replace natural gamma logging [7]. Schlumberger and other businesses launched an element capture spectroscopy logging (also known as formation element capture spectrum logging [ECS]) that detects secondary prompt gamma rays and ascertains the presence of rock-forming elements using the nuclear capture reaction of neutron radiation [8–10].

Small D-T neutron sources are affected by the D-T reaction's burn-up of tritium in the target, the natural loss caused by the tritium nucleus' natural decay, the working loss caused by the target's local overheating, and ion sputtering on its surface. As a result, the yield will keep declining [11]. Currently, it is required to determine the small D-T neutron source's yield in a neutron laboratory rather than on-site. It frequently depends on working hours while in use to decide if it can keep functioning. This will inevitably result in the premature replacement of some neutron sources before they reach the end of their useful lives, creating unnecessary waste; alternatively, some neutron tubes that have already reached the end of their useful lives may continue to function, producing abnormal test data and leading to mistakes in the processing and interpretation of the data. Therefore, it is essential to do yield detection.

D-T neutron source yield detection mainly includes associated particle method, activation method and neutron detector method. The associated particle method has the advantages of being highly accurate [12,13], but it is difficult to apply this technology in logging devices. The activation method is simple to use and has been used for power measurement of fusion and fission systems [14–16], but it requires long activation time and high fluxes to meet the requirements for neutron tube field detection. Neutron detector method like the ^{3}He, BF_3 detectors calculates the neutron yield by

* Corresponding author.
** Corresponding author.
E-mail addresses: xjzhang@ecut.edu.cn (X. Zhang), tangbin@ecut.edu.cn (B. Tang).

https://doi.org/10.1016/j.net.2023.03.013

detecting moderated thermal neutrons. When used for field measurements, it will be significantly affected by ambiently dispersed neutrons, which will lead to inaccuracy into the calculation of neutron source yield. As a result, we attempt to develop a new technology for figuring out D-T neutron source yields that may be used to field measurements. In this paper, a field determination method of D-T neutron source yields was proposed, which is a method of calculating the D-T neutron source yield through measuring the prompt gamma rays generated by bombarding oxygen with 14 MeV neutrons.

2. Oxygen prompt gamma rays method

D-T neutron source generates 14.1 MeV neutrons through the T (d, n)^{4}He process, which takes place when deuterons attack Triton. Strong monochromaticity characterizes the produced neutrons. The reaction formula is as follows.

$$^2_1H + ^3_1H = ^4_2He + ^1_0n + 17.6MeV$$

When fast neutrons interact with nuclei in the matter, nuclear reactions such as inelastic scattering (n, n' γ), elastic scattering (n, n), capture reactions (n,γ), and activating reactions occur. These nuclear processes cause incredibly quick-emitting gamma rays, which are known as prompt gamma rays [17,18]. By using a gamma ray detector to detect the prompt gamma ray and analyzing the data in accordance with the various gamma energies, the type and content of the elements in the substance can be determined.

Fast neutrons with energy more than 6 MeV can interact inelastically with oxygen ^{16}O (n,n')^{16}O*. When the excited state of ^{16}O* is deexcited, gamma rays with energies of 6.13 MeV, 6.92 MeV, and 7.12 MeV are produced. Fast neutrons with energy greater than 10.24 MeV can also activate oxygen ^{16}O (n,p)^{16}N. After beta decay, ^{16}N will create the excited ^{16}O nuclear state ^{16}O*, and ^{16}O* deexcitation will result in two gamma rays with energies of 6.13 MeV and 7.12 MeV. These two reactions lead to the oxygen prompt gamma rays. Oxygen prompt gamma rays method is the process of measuring oxygen prompt gamma rays in order to do physical analysis [19,20].

However, the application of the current oxygen prompt gamma rays method is used to determine the oxygen content on the assumption that the flux of the D-T neutron source is known (or eliminating the influence of the flux by an indirect method). Conversely, if the oxygen concentration of the material is constant, the oxygen prompt gamma rays method can be used to gather the pertinent information of the D-T neutron source.

3. Neutron-gamma radiation field transport equation

3.1. Source neutron diffusion equation

The D-T neutron source can be thought of as a point neutron source that continuously generates 14 MeV fast neutrons. The origin of the cylindrical coordinate system is used to determine the position of the point source, which is put in a homogenous oxygen-containing medium. The diffusion equation can be expressed using Eq. (1).

$$\frac{d^2\varphi(r)}{dr^2} + \frac{2}{r}\cdot\frac{d\varphi(r)}{dr} - \frac{\varphi(r)}{L_D^2} = 0 \quad (r \geq 0) \tag{1}$$

Since the neutron energy reacting with oxygen can be thought of as a one-speed neutron, the diffusion equation of the source neutron is found by solving Eq. (1) [21].

$$\varphi(r) = \frac{S}{4\pi Dr}e^{-r/L_D} \tag{2}$$

where $\varphi(r)$ is the neutron flux density at any point in the homogeneous medium; S is the neutron flux, or neutron source yield; r is the distance between the source point and the determination point; L_D is the diffusion length of one-speed neutrons in the medium; D is the diffusion coefficient of one-speed neutrons in the medium.

3.2. Oxygen prompt gamma rays field transport equation

The oxygen-containing medium is a cylinder with a radius of R_{CY} and a height of Z_{CY}, as shown in Fig. 1. The detector D lies in a plane with the horizontal section of the cylinder at a distance of d from the origin point, and its cylindrical coordinate is $(d,0,0)$. Given that the cylindrical coordinate of any point P in the oxygen-containing medium is (ρ, α, z), and that the emission point of the D-T neutron source is taken as the coordinate origin O, the neutron flux density at point P is given by Eq. (3).

$$\varphi_1\left(\overrightarrow{\mathbf{OP}}\right) = \frac{S}{4\pi D\sqrt{\rho^2+z^2}}e^{-\sqrt{\rho^2+z^2}/L_D} \tag{3}$$

The total microscopic cross section of the collision between the oxygen atoms in the medium and the source neutron to produce prompt gamma rays is σ, and the number of oxygen atoms in the medium is N. At point P, the source neutron's oxygen prompt gamma-ray reaction rate is $R(P)$.

$$R(P) = \frac{N\sigma S(1-A)}{4\pi D\sqrt{\rho^2+z^2}}e^{-\sqrt{\rho^2+z^2}/L_D} \tag{4}$$

where A is a constant associated with an oxygen-containing material , representing the possibility that the neutron source interacts with other elements other than oxygen at position P.

The secondary gamma field of oxygen prompt gamma rays will be generated at point P. Due to the high energy of oxygen prompt gamma rays (>6 MeV), the linear attenuation coefficient μ in the oxygen-containing medium can be regarded as being equivalent to that in the air. Then the flux rate of the oxygen prompt gamma rays generated at point P at detector point D can be calculated by Eq. (5).

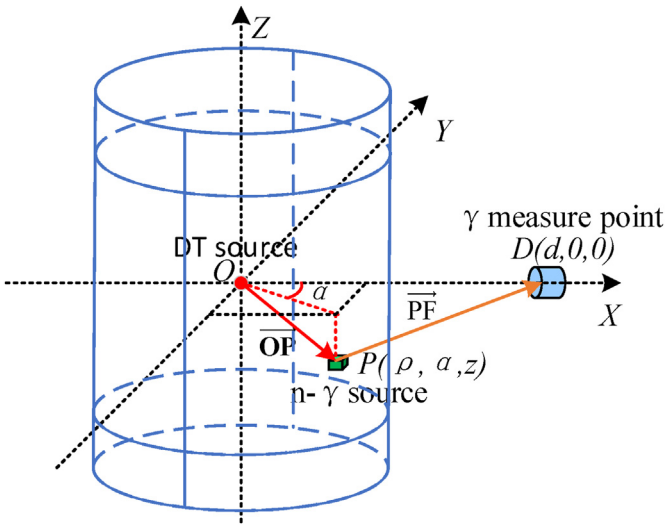

Fig. 1. Schematic diagram of n- γ radiation field transport.

$$\varphi_\gamma\left(\overrightarrow{\mathbf{PD}}\right)=\frac{N\sigma S(1-A)}{4\pi D\sqrt{\rho^2+z^2}}e^{-\sqrt{\rho^2+z^2}/L_D}\bullet\frac{1}{4\pi d_{PD}^2}e^{-\mu d_{PD}} \tag{5}$$

The length d_{PD} of $\overrightarrow{\mathbf{PD}}$ can be calculated using the geometry of the source point O, point P, and detector point D.

$$d_{PD}^2=(\rho\cos\alpha-d)^2+\rho^2\sin^2\alpha+z^2 \tag{6}$$

Eq. (5) can be expressed as the following when combined with Eq. (6).

$$\varphi_\gamma(d_{PD})=\frac{N\sigma S(1-A)}{4\pi D\sqrt{\rho^2+z^2}}e^{-\sqrt{\rho^2+z^2}/L_D}\bullet\frac{1}{4\pi\left[(\rho\cos\alpha-d)^2+\rho^2\sin^2\alpha+z^2\right]}e^{-\mu\sqrt{r(\rho\cos\alpha-d)^2+\rho^2\sin^2\alpha+z^2}} \tag{7}$$

Ignoring the influence of oxygen in the air (or deducting it as the background radiation), the count rate N_γ of oxygen prompt gamma rays measured by the detector can be calculated by Eq. (8).

$$N_\gamma=\int_{-\frac{Z_{CY}}{2}}^{\frac{Z_{CY}}{2}}\int_0^{2\pi}\int_0^{R_{CY}}\frac{N\sigma S(1-A)}{4\pi D\sqrt{\rho^2+z^2}}e^{-\sqrt{\rho^2+z^2}/L_D}\bullet\frac{1}{4\pi\left[(\rho\cos\alpha-d)^2+\rho^2\sin^2\alpha+z^2\right]}e^{-\mu\sqrt{r(\rho\cos\alpha-d)^2+\rho^2\sin^2\alpha+z^2}}d\rho d\alpha dz \tag{8}$$

According to Eq. (8), N_γ is proportional to the neutron source yield S when the oxygen-containing material are left unchanged. Eq. (8) can be rewritten as Eq. (9).

$$\begin{cases} N_\gamma=K\bullet S \\ K=\int_{-\frac{Z_{CY}}{2}}^{\frac{Z_{CY}}{2}}\int_0^{2\pi}\int_0^{R_{CY}}\frac{N\sigma(1-A)}{4\pi D\sqrt{\rho^2+z^2}}e^{-\sqrt{\rho^2+z^2}/L_D}\bullet\frac{1}{4\pi\left[(\rho\cos\alpha-d)^2+\rho^2\sin^2\alpha+z^2\right]}e^{-\mu\sqrt{r(\rho\cos\alpha-d)^2+\rho^2\sin^2\alpha+z^2}}d\rho d\alpha dz \end{cases} \tag{9}$$

where K is the conversion coefficient, which can be obtained from the standard neutron source experiment in addition to the integral calculation mentioned above. In this paper, K is obtained using the standard neutron source experiment.

4. Device for yield field determination and experimental platform

4.1. Device for yield field determination

The device for yield field determination adopts a ring structure, as shown in Fig. 2. The shell of the yield field determination device is made of aluminum. The basic components of the structure are a central cylinder, a loading cylinder, and a material pressure plate. The D-T neutron source is positioned inside the central cylinder, which has an inner diameter of 100 mm. The loading cylinder, which is the space between the center cylinder and the outer shell, is filled with powdered calcium oxide (CaO). Two thicknesses, 20 mm and 50 mm, with heights of 250 mm for both, were selected. To prevent oxygen-containing compounds from leaking, the material pressure plate is utilized to seal the loading cylinder.

4.2. Experimental test platform

The experiment was carried out at the China Institute of Atomic Energy. The neutron source is a Φ60mm small vertical D-T neutron source, and the neutron tube has a Penningion structure. The neutron source is controlled by adjusting the accelerating high voltage, filament current and ion source current of the neutron tube. The neutron source system and the control system are shown in Fig. 3, and the yield control parameters provided by the laboratory are shown in Table 1.

The gamma detector used was a 1024-channel gamma spectrometer developed by the East China University of Technology. A Φ50mm × 50 mm BGO ($Bi_4Ge_3O_{12}$) scintillation crystal was utilized as the probe. To reduce the influence of low-energy gamma ray scattering on the measuring results, a 5 mm-thick lead leather was installed in front of the probe. The experiment's environment is depicted in Fig. 4.

5. Testing and analysis

5.1. Oxygen prompt gamma spectra analysis

Two types of devices for determining the neutron yield with a thickness of 20 mm and 50 mm were tested on an experimental platform. The gamma energy spectra under different yields of the neutron source were obtained, as shown in Fig. 5. With an increase in the output of the neutron source, the spectral lines of gamma also increase in general, the characteristic peak of gamma 6.13 MeV becomes more obvious, and the characteristic peaks of 6.92 MeV and 7.12 MeV overlap. The measured energy spectra show obvious spectral drifting. The spectral lines should be adjusted before data processing using the spectral drifting correction method outlined in Ref. [22]. When calculating the neutron source yield using the energy segment analysis technique, the characteristic peak of 6.13 MeV, or the overlapping peaks of 6.92 MeV and 7.12 MeV, or the total energy area containing the three characteristic peaks of 6.13 MeV, 6.92 MeV and 7.12 MeV as three energy segments can be selected. The characteristic peak energy segment of 6.13 MeV gamma ray is called SCK(Fig. 5 (1)), and its energy range is 5.9 MeV–6.6 MeV. The overlapping peak energy segment of 6.92 MeV and 7.12 MeV gamma rays is called DCK(Fig. 5 (2)), and its energy range is 6.7 MeV–7.6 MeV. The total energy area is called TEA (Fig. 5 (3)), and its energy range is 5.9 MeV–7.6 MeV.

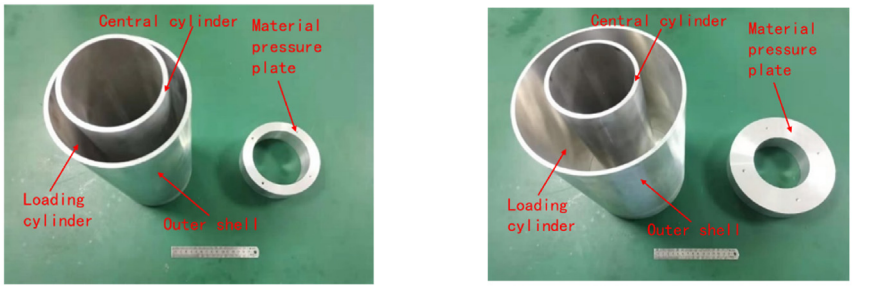

（a）device with a 20mm filling thickness （b）device with a 50mm filling thickness

Fig. 2. Actual photos of the device for yield field determination.

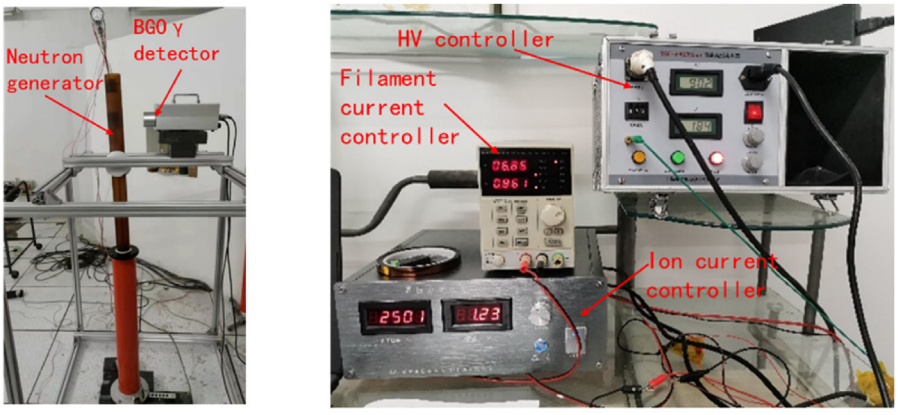

（a）Neutron source and gamma detectors （b）Neutron source control system

Fig. 3. Experimental test platform and control system.

Table 1
Yield control parameters of neutron source.

Yield/s^{-1}	High voltage/kV	Filament current/mA	Ion source current/μA
2.08×10^7	63	861	1070
3.96×10^7	73	861	1050
6.12×10^7	80	861	1020
7.92×10^7	86	861	960
1.00×10^8	90	861	950

5.2. Calculation of the conversion factor K

According to the energy spectra analysis, the division method of each energy segment was put forward in section 5.1. With four yield values of 2.08×10^7 s^{-1}, 3.96×10^7 s^{-1}, 6.12×10^7 s^{-1}, and 1.00×10^8 s^{-1}, each test point was measured for 3 min. Each of two field determination devices of different thickness were used. Then the conversion factor K can be obtained by applying the linear regression calculation method. Nevertheless, the oxygen prompt gamma count rate N_γ required in Eq. (9) is the net count rate generated by the determination device, and the background count rate brought by the measuring environment needs to be subtracted. And then Eq. (9) can be converted further into

$$S = \frac{1}{K} \bullet N_\gamma = \frac{1}{K} \bullet (N_{\gamma A} - N_B) \tag{10}$$

where $N_{\gamma A}$ is the total count rate of the oxygen prompt gamma rays; N_B is the environment background gamma count rate; the meaning of the remaining signals is the same as that given above.

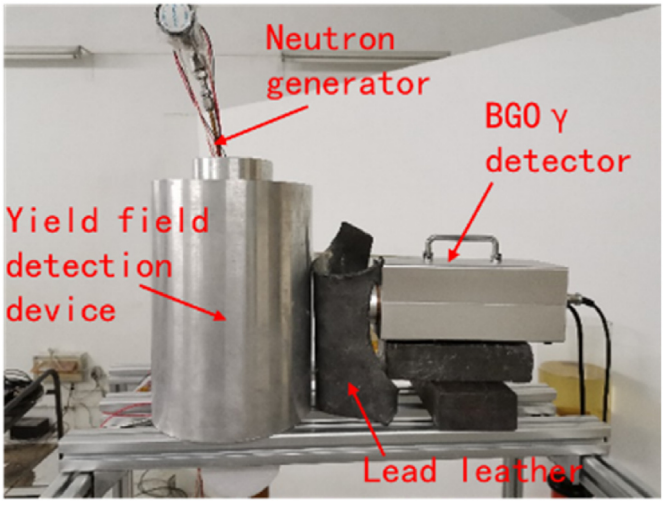

Fig. 4. Experiment's environment photo.

As shown in Fig. 6, the R-square of each calibration curve is higher than 94%. It demonstrates that the neutron yield is obviously linear with the prompt gamma count rate. This further confirms the feasibility of determining the D-T neutron source yield using oxygen prompt gamma rays.

Analyzing the conversion coefficients K of the two yield field determination devices, it can be seen that the three conversion

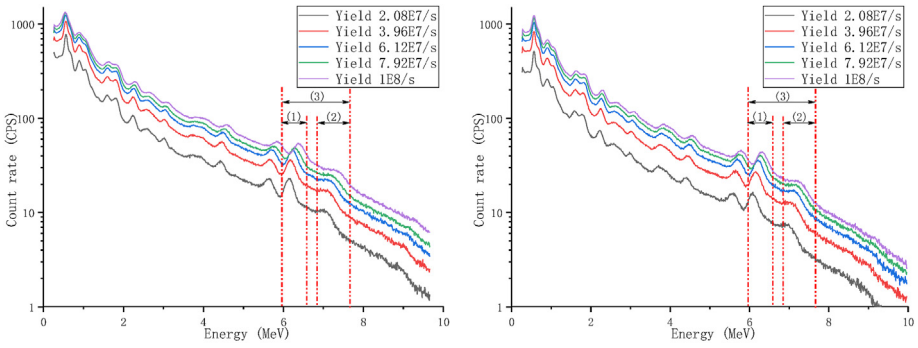

(a) Measured energy spectra of 20mm CaO yield field determination device

(b) Measured energy spectra of 50mm CaO yield field determination device

Fig. 5. Gamma spectra of two types of CaO yield field determination devices (1) SCK (2) DCK (3) TEA.

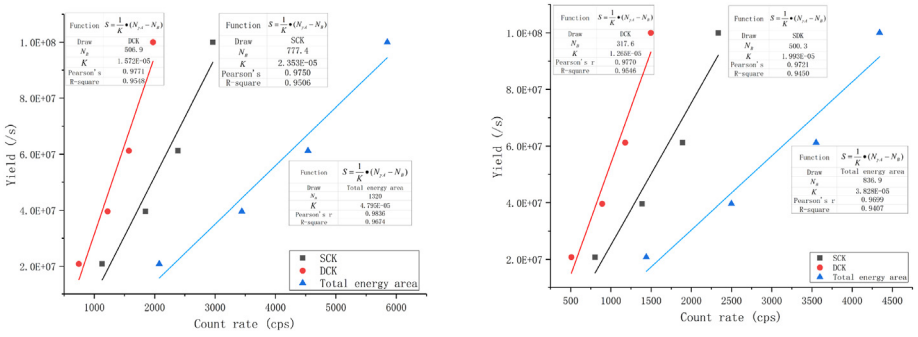

(a) Calibration curves of 20mm field determination device

(B) Calibration curves of 50mm field determination device

Fig. 6. Calibration curves of field determination devices.

Table 2
Yield test results of the two yield field determination devices.

D-T neutron source yield (s^{-1})	Device type	Data processing approaches	Count rate $N_{\gamma A}$ (cps)	Calculated yield (s^{-1})	Relative error
7.92×10^7	50 mm	SCK	2120.3	8.128 E+07	2.63%
		DCK	1371.7	8.333 E+07	5.21%
		TEA	3893.3	7.984 E+07	0.81%
	20 mm	SCK	2658.4	7.994 E+07	0.94%
		DCK	1784.8	8.129 E+07	2.64%
		TEA	5098.9	7.881 E+07	0.49%

coefficients K of the 50 mm device are respectively lower than those of the 20 mm device. It proves the sensitivity of the 50 mm determination device is better than that of the 20 mm device. In other words, the sensitivity of the determination device will improve as the oxygen content of the determination device increases.

The environment background gamma count rates N_B of the 50 mm device are all lower than those of the 20 mm device. This is because 50 mm device is thicker, less source neutron enters the environment. Lower environment background gamma count rate helps to reduce the detection limit of the device.

Additionally, as neutrons enter the environment, they could react with the oxygen in the BGO detector to create prompt gamma rays, which are likewise deposited in the detector and recorded. The existence of the aforementioned reaction is proved by the fact that the counting rate of the 20 mm device are higher than those of the 50 mm device in Table 2. Since the oxygen content of the BGO probe is also a constant, it can be considered that the oxygen content of the determination device has increased, maintaining the linear relationship between the prompt gamma rays and the neutron source yield. By using a standard neutron field experiment to calculate the conversion coefficient K, this effect can be eliminated.

Therefore, it is clear that raising the device's thickness and the mass of CaO will increase the device's sensitivity and decrease the device's detection limit. Additionally, it is reasonable to assume that this performance improvement is modest. In the subsequent research, the device's design should be optimized.

5.3. Test and analysis of neutron yield

Four of the five yields listed in Table 1 were chosen to determine

the conversion coefficient K. A yield of $7.92 \times 10^7 s^{-1}$ was set aside for testing the yield field determination device, and the measuring time was 3 min. The yield test results are shown in Table 2.

It can be seen from Table 2 that the relative errors of the three data processing approaches of the two yield field determination devices are all less than 10%. The maximum relative error is 5.21%, meeting the field quantitative requirements of conventional D-T neutron sources.

6. Conclusion

A field determination method of D-T neutron source yields based on oxygen prompt gamma rays was proposed. The neutron-gamma transport equation of the determination device was established. the accuracy of the method was confirmed through experiments.

(1) After fixing the mass of the oxygen-containing materials surrounding the D-T neutron source, the count rates of oxygen prompt gamma rays are proportional to the neutron yield. Therefore, a field method based on the oxygen prompt gamma rays was developed to determine the yield of a D-T neutron source.
(2) By establishing and analyzing the neutron-gamma transport equation of the determination device, its conversion coefficient *K* can be calculated by using multiple integrals or obtained through the standard neutron source experiment.
(3) Three methods—SCK, DCK, and TEA—were used to determine the count rates of the oxygen prompt gamma rays. The R-square of each method is superior to 94%. The maximum error of the yield test is 5.21%, demonstrating that it is feasible to estimate the yield of the D-T neutron source by using oxygen prompt gamma rays. It satisfies the field quantification requirements of the conventional D-T neutron source.
(4) The sensitivity and detection limit of the device can be improved by increasing the device's thickness and CaO mass. However, it is reasonable to assume that this performance improvement is modest. In the subsequent research, the device's design should be optimized.

Declaration of competing interest

The authors declare that they have no known competing financial interests or personal relationships that could have appeared to influence the work reported in this paper.

Acknowledgments

The authors would like to acknowledge the support of National Key R&D Program of China(2021YFC2900700); Nuclear Energy Development and Scientific Research Project(20201192–07); The National Natural Science Foundation of China(41704171); Joint Innovation Fund of China National Uranium Co., Ltd. and State Key Laboratory of Nuclear Resources and Environment (No. NRE2021-03).

Special thanks to Professor Liu Dan and Yang Linsen from the Institute of Nuclear Technology Application, China Institute of Atomic Energy, for their strong support for the experiment test.

References

[1] Feng Zhang, Summary of development for pulsed neutron well logging technology in our country [J], Chin. J. Atomic Energy Sci. Technol. (S1) (2009) 116–123.
[2] J. Batur, D. Sudac, V. Valkovic, I. Meric, H.E.S. Pettersen, K. Nad, M. Uroic, Z. Orlic, A. Perkovic, M. Gacina, J. Obhodas, Temporal and spatial resolution of the neutron probe for C/O nuclear well logging, Radiat. Phys. Chem. (2022), 110215.
[3] Jilin Fan, Feng Zhang, Lili Tian, Qixuan Liang, Xiaoyang Zhang, Qunwei Fang, Baoping Lu, Xianghui Li, A method of monitoring gas saturation in carbon dioxide injection heavy oil reservoirs by pulsed neutron logging technology, Petrol. Explor. Dev. 48 (6) (2021), 1420–142.
[4] L. Jacobson, R. Ethridge, G. Simpson, A new small diameter high-performance reservoir monitoring tool [C], in: The SPWLA 39th Annual Logging Symposium, 1998.
[5] Qian Chen, Feng Zhang, Fei Qiu, Zhen Wang, Yingming Liu, Quanying Zhang, Lili Tian, Jilin Fan, Qixuan Liang, Quantitatively determining gas content using pulsed neutron logging technique in closed gas reservoir, J. Petrol. Sci. Eng. 198 (2021), 108149.
[6] Zhang Yusheng, New well logging technology of determining reservoir saturation:PNN logging tool and its application, Chinese Journal of Petroleum Instruments 19 (3) (2005) 27–28.
[7] D.R. Humphreys, R.W. Barnard, H.M. Bivens, D.H. Jensen, W.A. Stephenson, J.H. Weinlein, Uranium logging with prompt fission neutrons, Appl. Radiat. Isot. 34 (1) (1983) 261–268.
[8] Schlumberger, ECS Elemental Capture Spectroscopy Sonde[EB/OL], 2006. http://www.slb. com/services/evaluation/wireline_open_hole/petrophysics/porosity/spectroscopy_sonde.aspx.
[9] Xugang Liu, Jianmeng Sun, Zhaocheng Li, A new generation of elemental capture spectroscopy logging, Chinese Journal of Isotope 15 (Z1) (2002) 8–13.
[10] Yuan Zu-Gui, Cheng Xiao-Ning, Juan Sun, ECS-new well-logging technique for completely evaluating the reservoir, Chinese Journal Atomic Energy Science and Technology (S1) (2004) 208–213.
[11] D. Partington, et al., Determination of the energy dependence of the ^{63}Cu $(n,2n)^{62}Cu$ and ^{27}Al $(n,p)^{27}Mg$ cross-sections, and their application to the measurement of 14-MeV neutron fluxes, Analyst 95 (1970) 257–259.
[12] J.C. Robertson, K.J. Zieba, On measuring the absolute yield of 14 MeV neutrons by associated particle counting, Nucl. Instrum. Methods 11 (1966) 179–180.
[13] Shifeng Sun, Xiaoping Ouyang, Study on angular resolution of associated particle fast neutron imaging system, Atomic Energy Sci. Technol. (5) (2020) 850–856.
[14] Vladimir Khripunov, Oxides for D–T neutron yield measurements by activation techniques on fusion devices, Fusion Eng. Des. 88 (2013) 1187–1191.
[15] Y. Uno, J. Kaneko, T. Nishitani, et al., Absolute measurement of D-T neutron flux with a monitor using activation of flowing water, Fusion Eng. Des. 56–57 (2001) 895–898.
[16] Ming Lei, Wenjie Zeng, et al., Measurement of HFETR reactor power by improved ^{16}N gamma spectrum analysis method, Ann. Nucl. Energy 164 (2021), 108604.
[17] Qing Shan, Shengnan Chu, Yongsheng Ling, et al., A neutron monitor for D-T neutron generator in the PGNAA-based online measurement system, Radiat. Phys. Chem. 135 (2017) 142–145.
[18] JiaTong Li, WenBao Jia, DaQian Hei, et al., Research on the optimization method for PGNAA system design based on Signal-to-Noise Ratio evaluation, Nucl. Eng. Technol. 54 (2022) 2221–2229.
[19] Marian Boromiza, et al., in: High precision neutron inelastic cross sections on ^{16}O[C]. EPJ Web of Conferences, EDP Sciences, 2020, 01013, https://doi.org/10.1051/epjconf/202023901013. https://hal.archives-ouvertes.fr/hal-02959054.
[20] D.R. Tilley, H.R. Weller, C.M. Cheves, Energy levels of light nuclei A = 16-17, Nucl. Phys. 565 (1993) 1–184.
[21] Xiting Lu, Nuclear Physics[M], Atomic Energy Press, 2000.
[22] Juan Zhai, Yuan Hu, Guo Cheng, Study of spectrum drifting correction method based on whole spectrum characteristic, Nucl. Electron. Detect. Technol. 37 (2017) 81–94.